Targeted alpha immunotherapy of CD20-positive B-cell lymphoma model: Dosimetry estimate of ^{225}Ac-DOTA-rituximab using ^{64}Cu-DOTA-rituximab

Chul-Hee Lee
Korea Institute of Radiological and Medical Sciences

Ilhan Lim (ilhan@kcch.re.kr)
https://orcid.org/0000-0002-5903-1659

Sang-Keun Woo
Korea Institute of Radiological and Medical Sciences

Wook Kim
Korea Institute of Radiological and Medical Sciences

Kwang Il Kim
Korea Institute of Radiological and Medical Sciences

Kyo Chul Lee
Korea Institute of Radiological and Medical Sciences

Kanghyon Song
Korea Institute of Radiological and Medical Sciences

Sang Moo Lim
Korea Institute of Radiological and Medical Sciences

Original research

Keywords: CD20-positive B-cell lymphoma, rituximab, 64Cu, PET, Monte Carlo simulation, 225Ac

Posted Date: July 2nd, 2020

DOI: https://doi.org/10.21203/rs.3.rs-26393/v2

Abstract

Background: To evaluate the radiation dosimetry of ^{225}Ac-DOTA-rituximab using Monte Carlo simulation of ^{64}Cu-DOTA-rituximab.

Methods: CD20 expression was evaluated in lymphoma cell lines (Jurkat and Raji). DOTA-rituximab was conjugated and then chelated by ^{64}Cu. Tumor xenograft models were established in BALB/c-nu mice. Animal PET/CT imaging was obtained after tail vein injection with and without a pre-dose of 2 mg of cold rituximab. Specific binding of tumors was evaluated by an organ distribution assay and autoradiography. CD20 expression in tumor tissues was evaluated by immunohistochemistry. The residence time was calculated using ^{64}Cu-DOTA-rituximab PET/CT acquisition data using OLINDA/EXM software. ^{225}Ac-DOTA-rituximab tumor dosimetry was performed using Monte Carlo simulation with ^{64}Cu-DOTA-rituximab PET/CT images.

Results: CD20 protein was highly expressed in Raji cells. Specific binding of Raji cells was 90 times that of Jurkat cells *($p<0.0001$).* Immunoreactivity was more than 75%. PET/CT imaging with ^{64}Cu-DOTA-rituximab was specifically observed in tumors. The radioactivity of the tumor was much higher than that of other organs, and tumor uptake was related to CD20 expression. The predicted human dose for the administration of ^{64}Cu-DOTA-rituximab was measured as the effective dose (1.07E-02 mSv/MBq). In the tumor region, equivalent doses of ^{225}Ac-DOTA-rituximab (14 Sv_{RBE5}/MBq) were much higher (74-fold) than those of ^{64}Cu-DOTA-rituximab (0.19 Sv_{RBE5}/MBq) (*$p<0.01$*).

Conclusion: Tumor dosimetry of ^{225}Ac-DOTA-rituximab can be estimated via the Monte Carlo simulation of ^{64}Cu-DOTA-rituximab. ^{225}Ac-DOTA-rituximab can be employed for lymphoma as targeted alpha therapy.

Introduction

Radioimmunotherapy (RIT) using beta-emitters such as ^{90}Y or ^{131}I has become an innovative method for B-cell non-Hodgkin's lymphoma (NHL) treatment **[1-3]**. Among these radiopharmaceuticals, ^{131}I-rituximab plays a role in treating patients with aggressive CD20-expressing B-cell NHL **[4-7]**. Our institute has used RIT for NHL patients using ^{131}I-rituximab **[8-12]**. RIT using ^{131}I-rituximab showed remarkable treatment results, but some patients experienced recurrence after RIT, which reveals resistance to the treatment. In this situation, more effective treatment modalities are required for better clinical outcomes.

Recently, targeted alpha therapy (TAT) was attempted and exhibited excellent results in certain diseases. TAT has been found to overcome resistance to beta emitters because the linear energy transfer (LET) of beta-emitters is low (0.1–1.0 keV/μm), while that of alpha-emitters (50–230 keV/μm) is high **[13]**. In this regard, it is a good strategy to apply rituximab RIT with alpha-emitter radionuclides such as Actinum-225 (^{225}Ac).

Ac-225 decays into ^{221}Fr, and finally to the more stable ^{209}Bi, yielding the four alpha-emitters **[14].** Some studies using the PSMA inhibitor, PSMA-617, demonstrated that ^{225}Ac-PSMA-617 contributes to the dramatic benefit in metastatic castration-resistant prostate cancer patients **[15, 16].** Other studies utilising antibodies also showed the effectiveness and safety of TAT **[17-19].** Accordingly, ^{225}Ac is a potent candidate for the radionuclide of RIT because its half-life of ^{225}Ac is 9.92 days **[20]** and rituximab has been known as an antibody with a long half-life, which is 2-7 days **[21].**

However, no study has evaluated ^{225}Ac-DOTA-rituximab in CD20-positive human B-cell lymphoma. In this study, we estimated the feasibility of RIT with ^{225}Ac-DOTA-rituximab in a CD20-positive B-cell lymphoma model through Monte Carlo simulation using ^{64}Cu-DOTA-rituximab. To perform this, we established a CD20-positive human lymphoma xenograft model to evaluate targeted imaging for non-invasive *in vivo* monitoring of lymphoma using ^{64}Cu-DOTA-rituximab PET and evaluated the correlation between CD20 expression and specific binding of ^{64}Cu-DOTA-rituximab in tumor tissue. For further studies, we estimated dosimetry using biodistribution results and quantitative analysis of ^{64}Cu-DOTA-rituximab PET imaging.

Materials And Methods

Antibody and Cell lines

CD20 targeted rituximab (Mabthera) was purchased from Roche. Human lymphoma cell lines (Jurkat and Raji) were used. Both cells were obtained from American Type Culture Collection (ATCC) and maintained in RPMI 1640 with 10% fetal bovine serum (Gibco) containing 1% antibiotics (penicillin G, 100 unitsmL, and streptomycin 10 μgml; Gibco). Cells were incubated at 37 °C in a 5% CO_2 atmosphere.

Western blot

Protein concentrations were determined using a BCA protein assay kit (Thermo Scientific). The membranes were blocked for 1 hour at room temperature and incubated with either anti-CD20 (#sc-58985) or β-actin (#A5441, Sigma-Aldrich) primary antibodies overnight at 4 °C. An enhanced chemical luminescence reagent (Roche) was used, and luminescent signals were measured with a ChemiDoc imaging system (Bio-Rad).

Immunoconjugation of DOTA-rituximab

For the desalting process of rituximab, we exchanged non-metallic D. W (D. W) using Amicon® ultra centrifugal filters (Millipore). The DOTA (1,4,7,10-tetraazacyclododecane-1,4,7,10tetraacetic acid)-NHS ester was purchased from FutureChem (#FC-2134, Seoul, Korea). Briefly, 10 mg rituximab was added to 200 μL of 1 M sodium bicarbonate (pH 8.0) for 5 min. DOTA-NHS (7 nM) was added to the mixture at 4 °C overnight. Excess DOTA-NHS ester was removed using a PD-10 column (GE Healthcare) using 1 mM sodium acetate buffer (pH 5.5). The number of chelators per antibody was calculated by matrix-assisted

laser desorption ionisation time-of-flight mass spectrometry (MALDI-TOF MS) to compare the molecular weights of DOTA-rituximab and rituximab.

Radiolabelling and Stability Tests

^{64}CuCl2 was produced at the Korea Institute of Radiological and Medical Sciences (Seoul, Korea) by 50 MeV cyclotron irradiation **[22]**. The ratio of $^{64}CuCl_2$ activity per DOTA-rituximab was determined to be 2 MBq per 1 mg. DOTA-rituximab conjugate was incubated with dried ^{64}CuCl2 in 1 mM sodium acetate buffer at 40 °C for 30 min. The radiolabelling yield was evaluated by instant thin-layer chromatography (iTLC) without additional purification. The stability of ^{64}Cu-DOTA-rituximab was analysed through iTLC after incubation in human and mouse serum, and phosphate buffered saline (PBS) at 37 °C for various times (1, 2, 6, 24, 48, and 60 h).

Cell binding assays and immunoreactivity

Cell binding with ^{64}Cu-DOTA-rituximab was performed using Jurkat and Raji cells. Both, Jurkat and Raji cell set-ups (5×10^5 cells /500 μL in tube) were incubated for 3 h in triplicate. Nonspecific binding (competitive inhibition) was performed by adding 11 μM of cold rituximab. After incubation, the cells were rinsed twice with cold PBS containing 1% bovine serum albumin (BSA). Cell bound radioactivity (count per minute) was evaluated using a γ-counter (Wizard 1480, Perkin-Elmer). Specific binding (%) was calculated using total binding and nonspecific binding data. To evaluate immunoreactivity **[23],** 3.1 nM of ^{64}Cu-DOTA-rituximab was added to Raji cells diluted from 1×10^7 cells/tube to 0.016×10^7 cells/tube in 500 μL serum-free medium. The incubation time, washing, and calculation methods were the same as above. The immunoreactive fraction was determined by performing a linear regression analysis of the double inverse plot of total/bound activity versus normalised cell concentration. The immunoreactive fraction was then obtained from the inverse of the intercept on the plot. Data analysis was performed using GraphPad Prism software.

Animal experiments

Six-week-old female BALB/c-nude mice were obtained from NARA Bio, Inc. All animal experiments were approved by the Institutional Animal Care and Use Committee of KIRAMS (2018-0061). For establishment of lymphoma xenograft mouse models (*n=5;* for PET/CT imaging, *n=3;* for biodistribution), Raji cells (5×10^7/ in 200 μL PBS) were transplanted subcutaneously into the right thigh. Small animal PET imaging and biodistribution studies were performed when tumor sizes were > 0.5 cm in diameter.

Small-animal PET/CT imaging

PET/CT images of tumor-bearing mice were acquired using PET/CT (INVEON scanner, Siemens Healthcare). Images were obtained for 20 min under inhalation anaesthesia (isoflurane, 1.5%) at 2, 24, and 48 h after intravenous injection (*i.v.*) of 7.4 – 7.7 MBq of ^{64}Cu-DOTA-rituximab per mouse. Blocking studies (*n=2*) were evaluated for CD20 specificity of ^{64}Cu-DOTA-rituximab. Non-labelled rituximab (10

mg/mL) was injected intravenously within 2 h before ^{64}Cu-DOTA-rituximab injection. To confirm the correlation with ^{64}Cu-DOTA-rituximab images, we injected 5.55 MBq of ^{18}F-FDG after more than 6 h food starvation. Images were reconstructed with INVEON software and the AMIDE algorithm (A Medical Image Data Examiner).

Biodistribution study

Biodistribution studies were performed to evaluate the uptake of ^{64}Cu-DOTA-rituximab in tumor-bearing mice or normal mice. All mice were intravenously injected with 1.85 MBq of ^{64}Cu-DOTA-rituximab. Tumor-bearing mice (*n=3*) were sacrificed 48 h after *i.v.* injection. For dosimetry, normal mice (*n=4*/group) were sacrificed at 1, 2, 6, 24, 48, and 72 h after *i.v.* injection. Various organs containing tumors and blood samples were weighed, and the radioactivity was measured. The γ-counter data were represented by the percentage of injected activity per gram of tissue (%IA/g).

Autoradiography and Immunofluorescence

After the γ-counting of tumors from the biodistribution study, tumor tissues were frozen using optimal cutting temperature (OCT) compound at -80 °C. A cryostat microtome (CM1800, Leica Instruments) was used for frozen sections of tumors tissue (15 μm depth in non-coating slide). The frozen sections were exposed on a film for 7 days in a deep freezer, and the film was scanned with BAS-5000 (Fujifilm). The image intensity of photostimulated luminescence was analysed using Fujifilm Multi Gauge software, version 3.0 (Fujifilm).

For immunostaining, a cryostat microtome was used for frozen sections of the tumors (7 μm depth in coating slide). Briefly, the slides were rinsed using PBS for 10 min and fixed in 4% paraformaldehyde for 10 min. After being washed twice, the slides were incubated in Triton X-100 for 10 min to permeate the tumors tissue. Normal goat serum (1%) was used for non-specific binding and incubated with anti-CD20 (#sc-58985) primary antibody overnight at 4 °C. To visualise specific binding of the antibody, fluorescence-labelled secondary anti-mouse antibody (Bethyl lab) was added to the slides for 1 h. Immunofluorescence images were obtained using IN Cell Analyzer 2200 (GE Healthcare).

Dosimetry calculation

Residence time was performed using the OLINDA/EXM software (Organ-Level Internal Dose Assessment/Exponential Modeling computer software, Vanderbilt University, 2003). The residence time was calculated at each time point for 2, 24, 48 h ^{64}Cu-DOTA-rituximab PET/CT acquisition data. The calculated region-of-interest (ROI) was defined based on the CT image. The ^{225}Ac-DOTA-rituximab tumor dosimetry was performed using Monte Carlo simulation with ^{64}Cu-DOTA-rituximab PET/CT tumor image. The absorbed dose of ^{225}Ac-DOTA-rituximab also considered all daughter radionuclides (^{221}Fr, ^{217}At, ^{213}Bi, ^{213}Po, ^{209}Tl, and ^{209}Pb) and summed up after applying weighting factors in the two possible pathways, 2% for ^{209}Tl and 98% for ^{213}Po.

S-value and Absorbed dose calculation

The specific tumor and organ S-value was acquired in Monte Carlo simulation from CT density information. CT density and PET radioactivity information were used as input data of Monte Carlo simulation. The S-value of the tumor and organs were calculated using simulated organ specific dose map. The S-value equation is as follows:

See formulas 1 and 2 in the supplmentary files.

Statistical analysis

All statistical analyses were performed using GraphPad Prism software. All data are evaluated as means ± standard deviation (SD) and are representative of at least two separate biological experiments performed in triplicate. Statistical significance between groups was compared using one-way ANOVA and unpaired Student's t-test. $P < 0.05$ was considered statistically significant.

Results

Specific CD20 targeting of ^{64}Cu-DOTA-rituximab

The mass difference between DOTA-rituximab and rituximab was about 1093 (m/z), and consequently we confirmed that the number of DOTA chelates per rituximab was approximately 2.8±0.21 **(Table S1)**. The radiolabeling efficiency was over 95% **(Figure S1.a),** and the stability of ^{64}Cu-DOTA-rituximab was over 90% in human and mouse serum, and in PBS **(Figure S1.b)**. CD20 expression was observed only in Raji cells **(Fig. 1a)**. Specific binding of ^{64}Cu-DOTA-rituximab in Raji cells was 90-fold higher than that in Jurkat cells *(p<0.0001)*. Between non-specific binding and total binding in Raji cells, the binding effect of ^{64}Cu-DOTA-rituximab was found to be significantly higher in total binding in Raji cells, by as much as 95-fold *(p<0.01)***(Fig. 1b, Table S2)**. Immunoreactivity was observed at 76%, which was similar to that observed in a study by Natarajan et al. **[25](Fig. 1c, d)**.

^{64}Cu-DOTA-rituximab PET/CT imaging in lymphoma models

To evaluate the *in vivo* PET imaging of lymphoma using ^{64}Cu-DOTA-rituximab, we established CD20-positive lymphoma xenograft models using Raji cells. Confirmation of the formation of the lymphoma model was done using ^{18}F-FDG. Localized ^{18}F-FDG uptake was observed at the xenograft site of the lymphoma model **(Figure S2)**. In the ^{64}Cu-DOTA-rituximab PET study, focal ^{18}F-FDG uptake was found in CD20 positive tumors at 24 h and 48 h (not shown at 2 h), but there was less uptake in the cold rituximab pre-injection group **(Fig. 2a)**. These uptake differences were remarkable at 48 h maximum intensity projection image from ^{64}Cu-DOTA-rituximab PET/CT **(Fig. 2b)**. In biodistribution results at 48 h, the distribution of ^{64}Cu-DOTA-rituximab in tumor groups revealed similar results, compared to the normal mice group without xenograft **(Fig. 2c)**. Autoradiography of the extracted tumor indicated a high correlation between autoradiography and immunohistochemistry with CD20 positive areas of the tumor

(Fig. 2d). Consequently, we demonstrated that ^{64}Cu-DOTA-rituximab specifically targeted CD20 positive tumors.

Equivalent dose calculation of ^{225}Ac-DOTA-rituximab using ^{64}Cu-DOTA-rituximab

To estimate the therapeutic effect of ^{225}Ac-DOTA-rituximab for targeted alpha-therapy using ^{64}Cu-DOTA-rituximab, S-values were calculated with both ^{64}Cu **[26]** and ^{225}Ac (data not shown) by means of Monte Carlo simulation with the CT images. The normal mice absorbed dose of ^{64}Cu-/^{225}Ac-DOTA-rituximab shown in **Table 1**. The equivalent dose (Sv_{RBE5}/MBq) of ^{64}Cu-/^{225}Ac-DOTA-rituximab in the heart, lung, liver, kidney, spleen, and tumor region was calculated. In the ^{64}Cu-DOTA-rituximab group, the highest equivalent dose was found in the tumor (0.19 Sv_{RBE5}/MBq), followed by the heart (0.14 Sv_{RBE5}/MBq) and lung (0.12 Sv_{RBE5}/MBq) **(Fig. 3a)**. On the other hand, the heart (34 Sv_{RBE5}/MBq) had the highest equivalent dose in the ^{225}Ac- DOTA-rituximab group **(Fig. 3b)**. With regards to the tumor equivalent dose, ^{225}Ac-DOTA-rituximab dose (14 Sv_{RBE5}/MBq) was 74 times the ^{64}Cu-DOTA-rituximab (0.19 Sv_{RBE5}/MBq) dose **(Fig. 3c)** ($p<0.01$).

Discussion

The current study aimed to evaluate radiation dosimetry for ^{225}Ac-DOTA-rituximab in CD20-positive B-cell lymphoma xenograft models. We demonstrated that ^{64}Cu-DOTA-rituximab specifically targeted CD20-positive lymphoma xenograft in terms of cell binding assay, biodistribution, autoradiography, and tissue staining as well as *in vivo* PET/CT imaging. In addition, we calculated the equivalent dose for ^{225}Ac-DOTA-rituximab TAT using Monte Carlo simulation of ^{64}Cu-DOTA-rituximab PET imaging.

The results of the present study correspond with those of a previous study, in which the biodistribution of ^{227}Th-DOTA-rituximab was similar to that of ^{64}Cu-DOTA-rituximab **[27-29]**. However, the equivalent dose of ^{227}Th-DOTA-rituximab (50 Sv_{RBE5}/MBq) **[27]** was lower than those of ^{64}Cu-DOTA-rituximab (0.19 Sv_{RBE5}/MBq), and ^{225}Ac -DOTA-rituximab (14 Sv_{RBE5}/MBq) because they are different radionuclides. Furthermore, these values were calculated using different methodologies. We maintain that this study's equivalent dose is more accurate than the radiation dose of ^{227}Th-DOTA-rituximab because the absorbed dose was estimated using the area under the curve of the time activity curve, **[27]** while this study analysed the equivalent dose using the tumor S value of the Monte Carlo simulation.

^{64}Cu-DOTA-rituximab was previously reported by Natarajan et al. as a radiopharmaceutical agent for diagnostic PET imaging **[25]**. This result was first presented from synthesis to dosimetry for human patients using a transgenic mouse model expressing huCD20 in the kidney. However, mouse xenograft models bearing human lymphoma cells were not studied using ^{64}Cu-DOTA-rituximab. Therefore, to obtain a tumor-targeting effect with organ distribution pattern of ^{64}Cu-DOTA-rituximab, we developed a CD20-positive lymphoma xenograft model. In our study, ^{64}Cu-DOTA-rituximab was also specifically bound to

only CD20 positive lymphoma cells **(Fig. 1)**. Furthermore, specific uptake in tumor was observed through PET/CT imaging, and the distribution pattern of ^{64}Cu-DOTA-rituximab in tumor models was evaluated **(Fig. 2)**. Additionally, we confirmed biodistribution and residence time in normal mice **(Figure S3).** In a normal biodistribution study, the half-life of ^{64}Cu-DOTA-rituximab in mouse blood was estimated to be approximately 6-21 h **[30]**. Consequently, these results suggest that ^{64}Cu-DOTA-rituximab specifically targets CD20-positive human B-cell lymphoma.

Generally, the pharmacokinetics of therapeutic radiopharmaceuticals are analysed using diagnostic radionuclides. For example, some studies prefer to use ^{124}I-mIBG PET/CT images for ^{131}I-mIBG targeted radionuclide therapy as a means for better treatment planning **[31]**. In addition, the radiation dosimetry of ^{213}Bi-PSMA-617 was estimated using ^{68}Ga-PSMA-617 imaging in patients for clinical application of alpha radionuclide therapy **[32]**. As a positron emitter, ^{64}Cu is also an attractive diagnostic radionuclide for PET imaging **[33]**. Using ^{64}Cu, Woo et al. calculated the absorbed dose of ^{67}Cu-DOTA/NOTA-trastuzumab to evaluate the therapeutic effect of HER2-positive breast cancer **[26]**. Based on this method, we estimated the radiation dosimetry of ^{225}Ac-DOTA-rituximab using ^{64}Cu-DOTA-rituximab PET/CT imaging from CD20-positive human B-cell lymphoma models **(Fig. 3)**. The OLINDA/EXM software is widely used for the analysis of normal organ dosimetry. However, this software has been used for human digitalised phantoms, and its limitation is that it cannot calculate abnormal regions such as the tumor region. For this reason, we performed a Monte Carlo simulation to calculate the absorbed dose in the tumor regions. Our results demonstrated that ^{225}Ac-DOTA-rituximab showed a significantly larger equivalent dose than ^{64}Cu-DOTA-rituximab **(Fig. 3c)**. Consequently, a low dose of ^{225}Ac-DOTA-rituximab can be applied to provide targeted therapy by releasing high LET alpha-emitters.

High LET alpha particles are promising candidates for killing target cells. Among them, ^{225}Ac plays an important role in TAT and can be used efficiently and safely **[34]**. Some studies have shown that high energy within a short range induces DNA damage at least 100-fold higher than beta particles **[35]**, and DNA double strand breakage (DSB) has therapeutic effects **[36]**. With regard to radiation dose, another study revealed that the radiation dose (Gy/Bq) of ^{225}Ac was 900 times that of lutetium-177 (^{177}Lu) and 14 times that of radium-223 (^{223}Ra) through Monte Carlo simulation **[37]**. This result could explain why equivalent doses of ^{225}Ac-DOTA-rituximab in major organs were higher than those of ^{64}Cu-DOTA-rituximab and tumor **(Fig. 3a, b)**. Similarly, TAT using ^{225}Ac-DOTATOC triggers much higher γH2AX-foci formation from DSB than ^{177}Lu-DOTATOC **[37]**. Therefore, we can infer that ^{25}Ac-DOTA-rituximab could be a more effective treatment option than ^{131}I-rituximab for NHL patients. We have performed a clinical trial of RIT for NHL patients using ^{131}I-rituximab for 16 years **[8-12]**. RIT demonstrated excellent results, but some refractory patients showed resistance to RIT. We expect that it is necessary to treat these refractory patients using more powerful RIT agents. We calculated the probable radiation dose to the tumor and found that ^{225}Ac-DOTA-rituximab revealed a higher radiation dose to the tumor than ^{131}I-rituximab.

Our study has several limitations. First, we analysed only the ^{64}Cu-DOTA-rituximab results in terms of biological experiments. To evaluate the therapeutic effect of ^{225}Ac-DOTA-rituximab more precisely, we need further studies using ^{225}Ac-DOTA-rituximab radiopharmaceutical using an *in vivo* tumor model. Furthermore, clinical trials are warranted to verify the adverse effects and therapeutic effects of ^{225}Ac-DOTA-rituximab. Fortunately, some studies demonstrated that biodistribution patterns using trastuzumab were significantly related between ^{64}Cu-DOTA and ^{225}Ac -DOTA groups in murine models **[38, 39]**. Watabe T et al. **[40]** also observed that ^{64}Cu/^{225}Ac-FAPI-04 in murine tumor model had a similar trend according to physiological accumulation. These results could be supported our hypothesis that appropriateness of ^{64}Cu as a surrogate marker of ^{225}Ac. Second, while it has been considered that the lymphoma transgenic mice model will be more clinically relevant than the lymphoma xenograft model, we still preferred to utilise the CD20-positive B-cell lymphoma xenograft model due to the difficulty in evaluating the radiation dosimetry using the small tumor from transgenic mice models. Hopefully, we succeeded in labelling the ^{225}Ac-DOTA-rituximab group (data not shown). In addition, comparison of the therapeutic effect of ^{131}I-rituximab and ^{225}Ac-DOTA-rituximab is ultimately required to confirm the cytotoxicity.

Conclusion

Tumor dosimetry of ^{225}Ac-DOTA-rituximab can be estimated via the Monte Carlo simulation of ^{64}Cu-DOTA-rituximab. ^{225}Ac-DOTA-rituximab can be employed for lymphoma as targeted alpha therapy.

Declarations

Acknowledgements

Not applicable

Author’s contributions

This study was designed by Chul-Hee Lee, Ilhan Lim, Sang-Keun Woo, Wook Kim, Kwang Il Kim, Kyo Chul Lee, Kanghyon Song, and Sang Moo Lim. Data acquisition and analysis was performed by Chul-Hee Lee, Wook Kim, and Sang-Keun Woo. Chul-Hee Lee and Ilhan Lim wrote the manuscript draft. All authors reviewed and edited this final version of the manuscript.

Funding

This study was supported by a grant from the Korea Institute of Radiological and Medical Sciences (KIRAMS), funded by the Ministry of Science and ICT, Republic of Korea (No. 50547-2020) and the National Research Foundation of Korea (NRF) grant funded by the Korea government (Ministry of Science and ICT) (No. 2019M2D2A1A02057204)

Availability of data and material

The data underlying the analyses in this manuscript are available on demand from the author.

Ethics approval

This study was performed in accordance with the ethical standards of our institutions and with the 1964 Helsinki Declaration and its later amendments or comparable ethical standards.

Consent for publication

Not applicable.

Competing interests

The authors declare that they have no conflicts of interest.

Abbreviations

RIT: Radioimmunotherapy; NHL: Non-Hodgkin's lymphoma; TAT: Targeted alpha therapy; LET: Linear energy transfer; DOTA: 1,4,7,10-tetraazacyclododecane-1,4,7,10tetraacetic acid; BSA: Bovine serum albumin; %IA/g: Percentage of injected activity per gram of tissue; OLINDA/EXM software: Organ-Level Internal Dose Assessment/Exponential Modeling computer software; DSB: Double strand breakage

References

1. Hagenbeek A. Radioimmunotherapy for NHL: experience of ^{90}Y-ibritumomab tiuxetan in clinical practice. Leuk Lymphoma. 2003;44 Suppl 4:S37-47.
2. Kaminski MS, Estes J, Zasadny KR, Francis IR, Ross CW, Tuck M, Regan D, Fisher , et al., Radioimmunotherapy with iodine (131)I tositumomab for relapsed or refractory B-cell non-Hodgkin lymphoma: updated results and long-term follow-up of the University of Michigan experience. Blood. 2000;96:1259-66.
3. Kaminski MS, Tuck M, Estes J, Kolstad A, Ross CW, Zasadny K., et al., ^{131}I-tositumomab therapy as initial treatment for follicular lymphoma. N Engl J Med. 2005;352:441-9.
4. Bienert M, Reisinger I, Srock S, Humplik BI, Reim C, Kroessin T., et al., Radioimmunotherapy using ^{131}I-rituximab in patients with advanced stage B-cell non-Hodgkin's lymphoma: initial experience. Eur J Nucl Med Mol Imaging. 2005;32:1225-33.
5. Leahy MF, Seymour JF, Hicks RJ, Turner JH. Multicenter phase II clinical study of iodine-131-rituximab radioimmunotherapy in relapsed or refractory indolent non-Hodgkin's J Clin Oncol. 2006;24:4418-25.
6. Turner Defining pharmacokinetics for individual patient dosimetry in routine radiopeptide and radioimmunotherapy of cancer: Australian experience. Curr Pharm Des. 2009;15:966-82.

7. Kang HJ, Lee SS, Byun BH, Kim KM, Lim I, Choi CW., et al., Repeated radioimmunotherapy with ^{131}I-rituximab for patients with low-grade and aggressive relapsed or refractory B cell non-Hodgkin lymphoma. Cancer Chemother Pharmacol. 2013;71:945-53.
8. Kang GW, Kang HJ, Shin DY, Gu HR, Choi HS, Lim SM. Radioimmunotherapy with (131)i-rituximab in a patient with diffuse large B-cell lymphoma relapsed after treatment with (90)y-ibritumomab tiuxetan. Nucl Med Mol Imaging. 2013;47:281-4.
9. Kang HJ, Lee SS, Kim KM, Choi TH, Cheon GJ, Kim WS., et al., Radioimmunotherapy with (131)I-rituximab for patients with relapsed/refractory B-cell non-Hodgkin's lymphoma (NHL). Asia Pac J Clin Oncol. 2011;7:136-45.
10. Lee I, Byun BH, Lim I, Kim BI, Choi CW, Kim KM., et al., Comparisons of ^{131}I-rituximab treatment responses in patients with aggressive lymphoma and indolent lymphoma. Ann Nucl Med. 2019;33:881-90.
11. Lim I, Park JY, Kang HJ, Hwang JP, Lee SS, Kim KM., et al., Prognostic significance of pretreatment ^{18}F-FDG PET/CT in patients with relapsed/refractory B-cell non-Hodgkin's lymphoma treated by radioimmunotherapy using ^{131}I-rituximab. Acta Haematol. 2013;130:74-82.
12. Shin DY, Byun BH, Kim KM, Kang JH, Lim I, Kim BI., et al., Radioimmunotherapy with (131)I-rituximab as consolidation therapy for patients with diffuse large B-cell lymphoma. Cancer Chemother Pharmacol. 2016;78:825-31.
13. Seidl C. Radioimmunotherapy with α-particle-emitting radionuclides. Immunotherapy. 2014;6:431-58.
14. McDevitt MR, Sgouros G, Finn RD, Humm JL, Jurcic JG, Larson SM., et al., Radioimmunotherapy with alpha-emitting nuclides. Eur J Nucl Med. 1998;25:1341-51.
15. Essler M, Gärtner FC, Neff F, Blechert B, Senekowitsch-Schmidtke R, Bruchertseifer F., et al., Therapeutic efficacy and toxicity of ^{225}Ac-labelled vs. ^{213}Bi-labelled tumour-homing peptides in a preclinical mouse model of peritoneal carcinomatosis. Eur J Nucl Med Mol Imaging. 2012;39:602-12.
16. Kratochwil C, Bruchertseifer F, Giesel FL, Weis M, Verburg FA, Mottaghy F., et al., ^{225}Ac-PSMA-617 for PSMA-Targeted α-Radiation Therapy of Metastatic Castration-Resistant Prostate Cancer. J Nucl Med. 2016;57:1941-4.
17. Sgouros G, Roeske JC, McDevitt MR, Palm S, Allen BJ, Fisher DR., et al., MIRD Pamphlet No. 22 (abridged): radiobiology and dosimetry of alpha-particle emitters for targeted radionuclide therapy. J Nucl Med. 2010;51:311-28.
18. Borchardt PE, Yuan RR, Miederer M, McDevitt MR, Scheinberg DA. Targeted actinium-225 in vivo generators for therapy of ovarian cancer. Cancer Res. 2003;63:5084-90.
19. Behling K, Maguire WF, López Puebla JC, Sprinkle SR, Ruggiero A, O'Donoghue J., et al., Vascular Targeted Radioimmunotherapy for the Treatment of Glioblastoma. J Nucl Med. 2016;57:1576-82.
20. Pommé S, Marouli M, Suliman G, Dikmen H, Van Ammel R, Jobbágy V., et al., Measurement of the ^{225}Ac half-life. Appl Radiat Isot. 2012;70:2608-14.

21. Reff ME, Carner K, Chambers KS, Chinn PC, Leonard JE, Raab R., et al., Depletion of B cells in vivo by a chimeric mouse human monoclonal antibody to CD20. Blood. 1994;83:435-45.
22. Kim JY, Park H, Lee JC, Kim KM, Lee KC, Ha HJ., et al., Simple Cu-64 production and its application of Cu-64 ATSM. Appl Radiat Isot. 2009;67:1190-4.
23. Lindmo T, Boven E, Cuttitta F, Fedorko J, Bunn Jr PA. Determination of the immunoreactive function of radiolabeled monoclonal antibodies by linear extrapolation to binding at infinite antigen excess. J Immunol Methods. 1984;72:77-89.
24. Snyder "S" absorbed dose per unit cumulated activity for selected radionuclides and organs. MIRD Pamphlet no. 11. 1975.
25. Natarajan A, Gowrishankar G, Nielsen CH, Wang S, Iagaru A, Goris ML., et al., Positron emission tomography of ^{64}Cu-DOTA-Rituximab in a transgenic mouse model expressing human CD20 for clinical translation to image NHL. Mol Imaging Biol. 2012;14:608-16.
26. Woo SK, Jang SJ, Seo MJ, Park JH, Kim BS, Kim EJ., et al., Development of ^{64}Cu-NOTA-Trastuzumab for HER2 Targeting: A Radiopharmaceutical with Improved Pharmacokinetics for Human Studies. J Nucl Med. 2019;60:26-33.
27. Dahle J, Borrebaek J, Jonasdottir TJ, Hjelmerud AK, Melhus KB, Bruland ØS., et al., Targeted cancer therapy with a novel low-dose rate alpha-emitting radioimmunoconjugate. Blood. 2007;110:2049-56.
28. Dahle J, Borrebaek J, Melhus KB, Bruland OS, Salberg G, Olsen DR., et al., Initial evaluation of (227)Th-p-benzyl-DOTA-rituximab for low-dose rate alpha-particle radioimmunotherapy. Nucl Med Biol. 2006;33:271-9.
29. Dahle J, Bruland OS, Larsen RH. Relative biologic effects of low-dose-rate alpha-emitting ^{227}Th-rituximab and beta-emitting ^{90}Y-tiuexetan-ibritumomab versus external beam X-radiation. Int J Radiat Oncol Biol Phys. 2008;72:186-92.
30. McLaughlin P, Grillo-López AJ, Link BK, Levy R, Czuczman MS, Williams ME., et al., Rituximab chimeric anti-CD20 monoclonal antibody therapy for relapsed indolent lymphoma: half of patients respond to a four-dose treatment program. J Clin Oncol. 1998;16:2825-33.
31. Huang SY, Bolch WE, Lee C, Van Brocklin HF, Pampaloni MH, Hawkins RA., et al., Patient-specific dosimetry using pretherapy [^{124}I]m-iodobenzylguanidine ([^{124}I]mIBG) dynamic PET/CT imaging before [^{131}I]mIBG targeted radionuclide therapy for neuroblastoma. Mol Imaging Biol. 2015;17:284-94.
32. Kratochwil C, Schmidt K, Afshar-Oromieh A, Bruchertseifer F, Rathke H, Morgenstern A., et al., Targeted alpha therapy of mCRPC: Dosimetry estimate of ^{213}Bismuth-PSMA-617. Eur J Nucl Med Mol Imaging. 2018;45:31-7.
33. Wadas TJ, Wong EH, Weisman GR, Anderson CJ. Copper chelation chemistry and its role in copper radiopharmaceuticals. Curr Pharm Des. 2007;13:3-16.
34. McDevitt MR, Ma D, Lai LT, Simon J, Borchardt P, Frank RK., et al., Tumor therapy with targeted atomic nanogenerators. Science. 2001;294:1537-40.

35. Sgouros G, Hobbs RF. Dosimetry for radiopharmaceutical therapy. Semin Nucl Med. 2014;44:172-8.
36. Couturier O, Supiot S, Degraef-Mougin M, Faivre-Chauvet A, Carlier T, Chatal JF., et al., Cancer radioimmunotherapy with alpha-emitting nuclides. Eur J Nucl Med Mol Imaging. 2005;32:601-14.
37. Azorín-Vega E, Rojas-Calderón E, Ferro-Flores G, Aranda-Lara L, Jiménez-Mancilla N, Nava-Cabrera MA. Assessment of the radiation absorbed dose produced by ^{177}Lu-iPSMA, ^{225}Ac-iPSMA and ^{223}RaCl2 to prostate cancer cell nuclei in a bone microenvironment model. Appl Radiat Isot. 2019;146:66-71.
38. Paudyal P, Paudyal B, Hanaoka H, Oriuchi N, Iida Y, Yoshioka H., et al., Imaging and biodistribution of Her2/neu expression in non-small cell lung cancer xenografts with Cu-labeled trastuzumab PET. Cancer Sci. 2010;101:1045-50.
39. Li L, Rousseau J, Jaraquemada-Peláez MG, Wang X, Robertson A, Radchenko V., et al., ^{225}Ac-H4py4pa for Targeted Alpha Therapy. Bioconjug Chem. 2020; doi: 10.1021/acs.bioconjchem.0c00171.
40. Watabe T, Liu Y, Kaneda-Nakashima K, Shirakami Y, Lindner T, Ooe K., et al., Theranostics Targeting Fibroblast Activation Protein in the Tumor Stroma: ^{64}Cu- and ^{225}Ac-Labeled FAPI-04 in Pancreatic Cancer Xenograft Mouse Models. J Nucl Med. 2020;61:563-569.

Table

Table 1. Normal organ absorbed dose of ^{64}Cu-/^{225}Ac-DOTA-rituximab in mice

	^{64}Cu-DOTA-Rituximab Absorbed dose (mGy/MBq)		^{225}Ac-DOTA-Rituximab Absorbed dose (mGy/MBq)	
	Mean	SD	Mean	SD
Stomach Wall	7.23E-03	3.04E-03	1.48E+00	9.17E-01
Heart Wall	2.33E-02	1.43E-02	5.52E+00	3.36E+00
Kidneys	4.04E-02	2.52E-02	9.84E+00	6.14E+00
Liver	4.06E-02	3.03E-02	9.51E+00	7.13E+00
Lungs	5.56E-02	4.34E-02	5.88E+00	4.60E+00
Spleen	3.53E-02	2.22E-02	9.11E+00	5.73E+00
Effective dose (mSv/MBq)	1.07E-02	7.06E-03	2.17E+00	1.36E+00

Figures

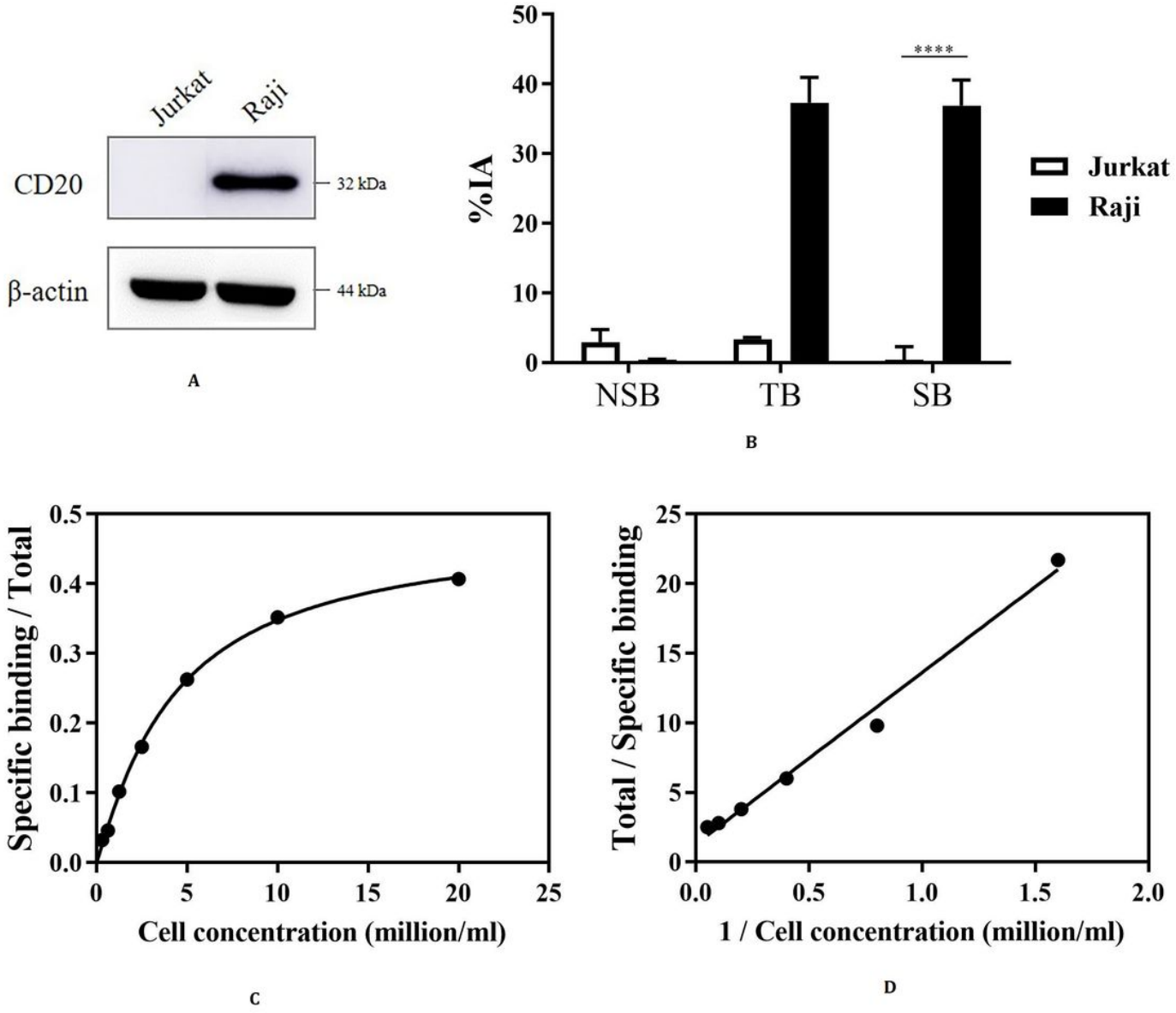

Figure 1

CD20 expression and 64Cu-DOTA-ritxuaimb binding a Western blot analysis of CD20. β-actin was used as an internal control. CD20 expression was observed in Raji cells. b Cell binding assay of 64Cu-DOTA-rituximab Specific binding (SB) of Raji cells was 90-fold higher than that of Jurkat cells ($p<0.0001$). c and d Immunoreactivity assay (Lindmo assay) using Raji cells. d was analysed using GraphPad software from c. Immunoreactivity was 76%

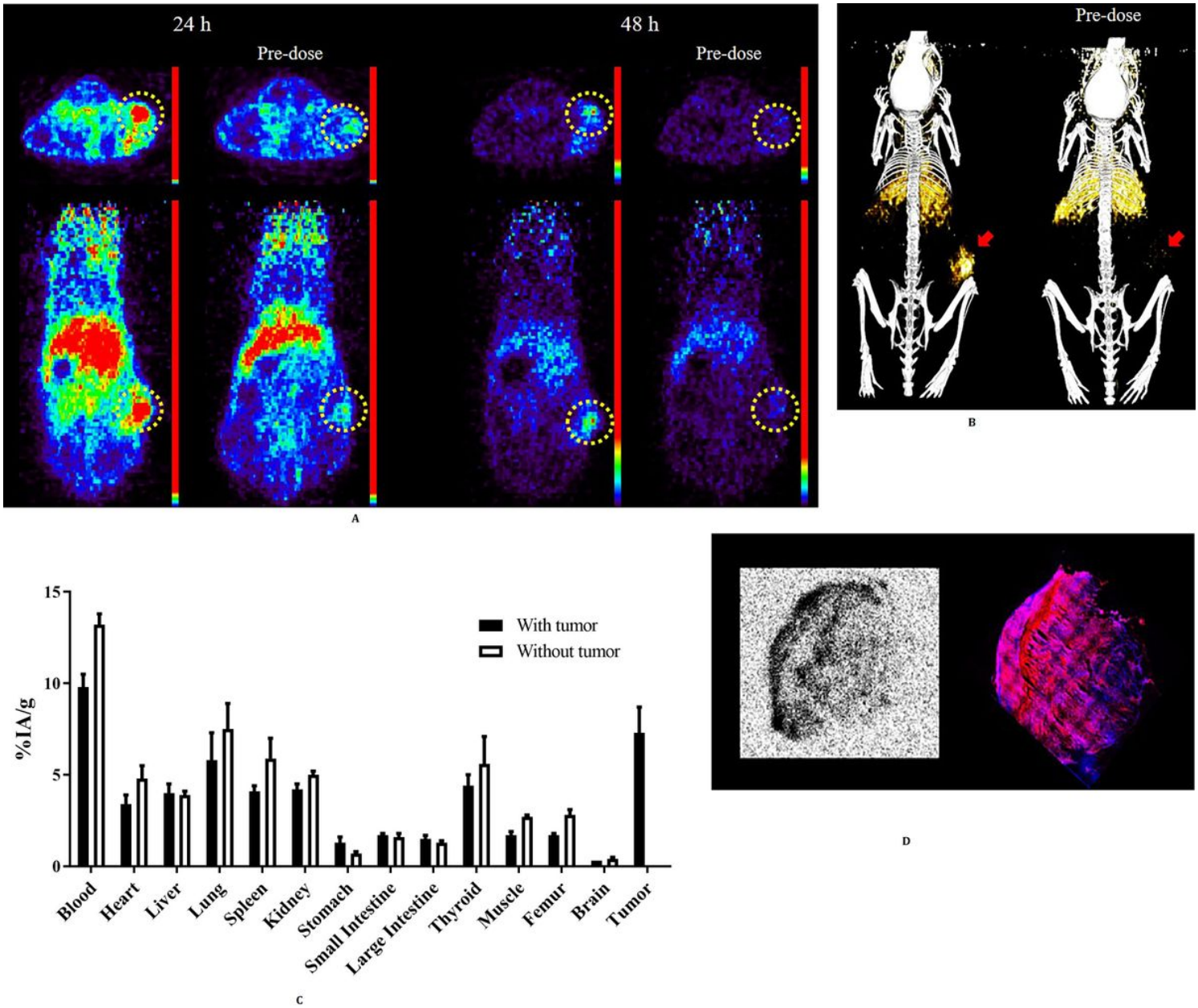

Figure 2

In vivo lymphoma models and 64Cu-DOTA-rituximab PET/CT imaging a 64Cu-DOTA-rituximab PET imaging at 24 and 48 h with (n=2) and without (n=3) blocking by cold-rituximab. b Representative PET/CT imaging at 48 h using 3D visualisation software. Tumor-targeted imaging was observed. c Biodistribution study with (n=3) and without (n=4) lymphoma at 48 h. Accumulation in the tumor was the second highest. d Autoradiography (64Cu-DOTA-rituximab) and immunostaining (CD20) images showed a correlation

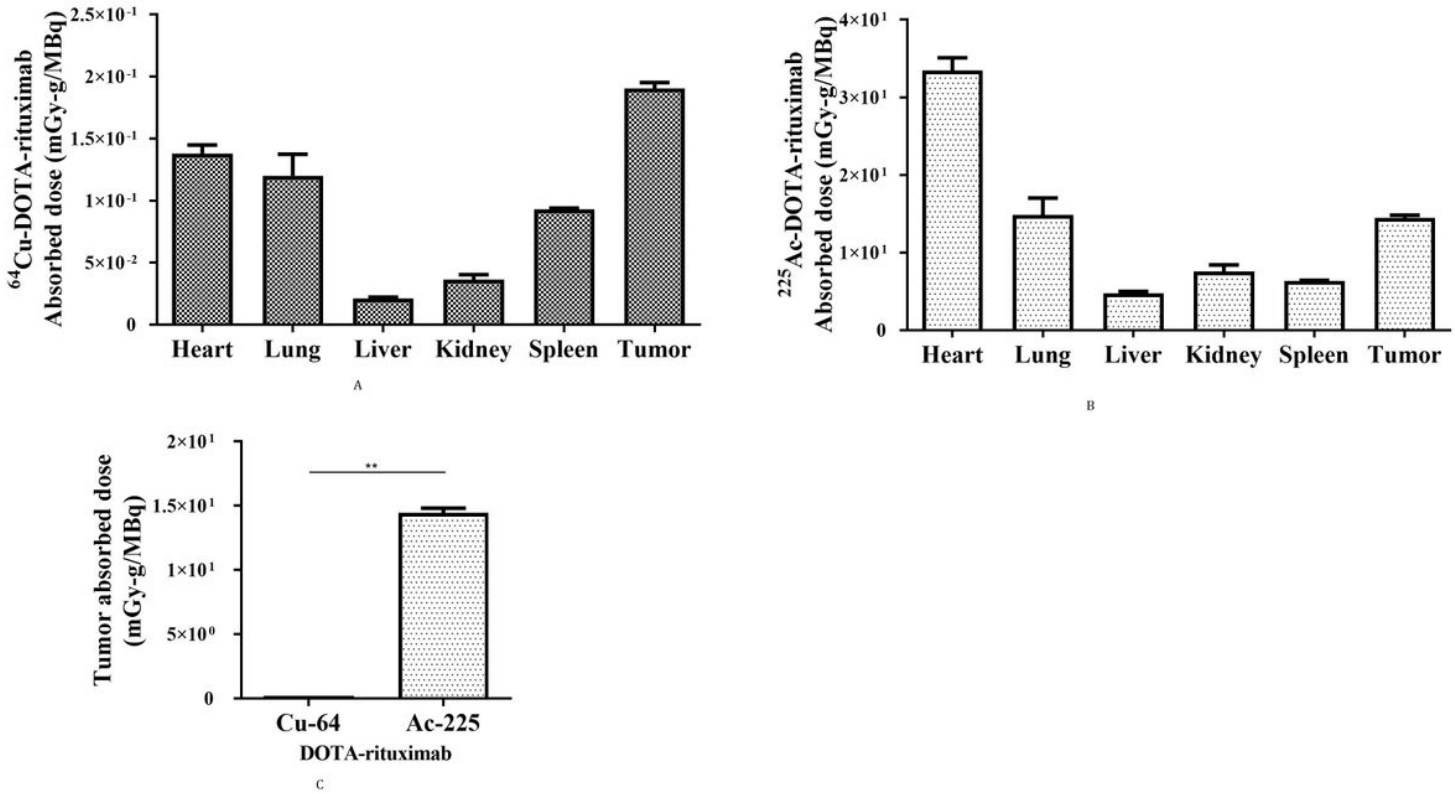

Figure 3

Absorbed dose estimation of 64Cu- and 225Ac-DOTA-rituximab using Monte Carlo simulation. a Absorbed dose of 64Cu-DOTA-rituximab in mouse tumor model. b Absorbed dose of 225Ac-DOTA-rituximab in mouse tumor model. c Relative absorbed dose in tumors of Cu-64 or Ac-225 ($P < 0.01$). Data were obtained from a and b

Supplementary Files

This is a list of supplementary files associated with this preprint. Click to download.

- SupplementaryFig1200630.docx
- SupplementaryTable1.docx
- SupplementaryFig2200630.docx
- SupplementaryFig3200630.docx